Supplement of Clim. Past, 22, 1609–1629, 2026
https://doi.org/10.5194/cp-22-1609-2026-supplement

Supplement of

Mixed layer depth in the PMIP4 *midHolocene* simulations: comparison to proxy data in North Atlantic deep convection regions

Xiner Wu et al.

Correspondence to: Xiner Wu (wu.xiner@courrier.uqam.ca)

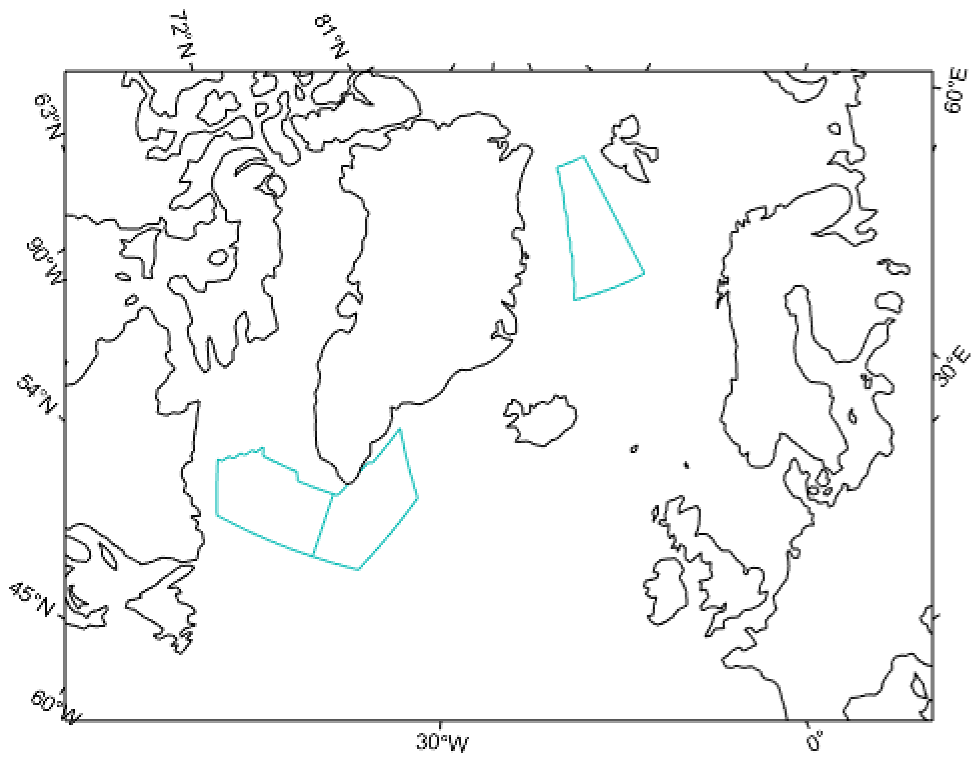

Figure S1. Three regions of deep-water formation used for averaging the simulated MLDs (the Labrador Sea, the Irminger Sea, the Greenland Sea).

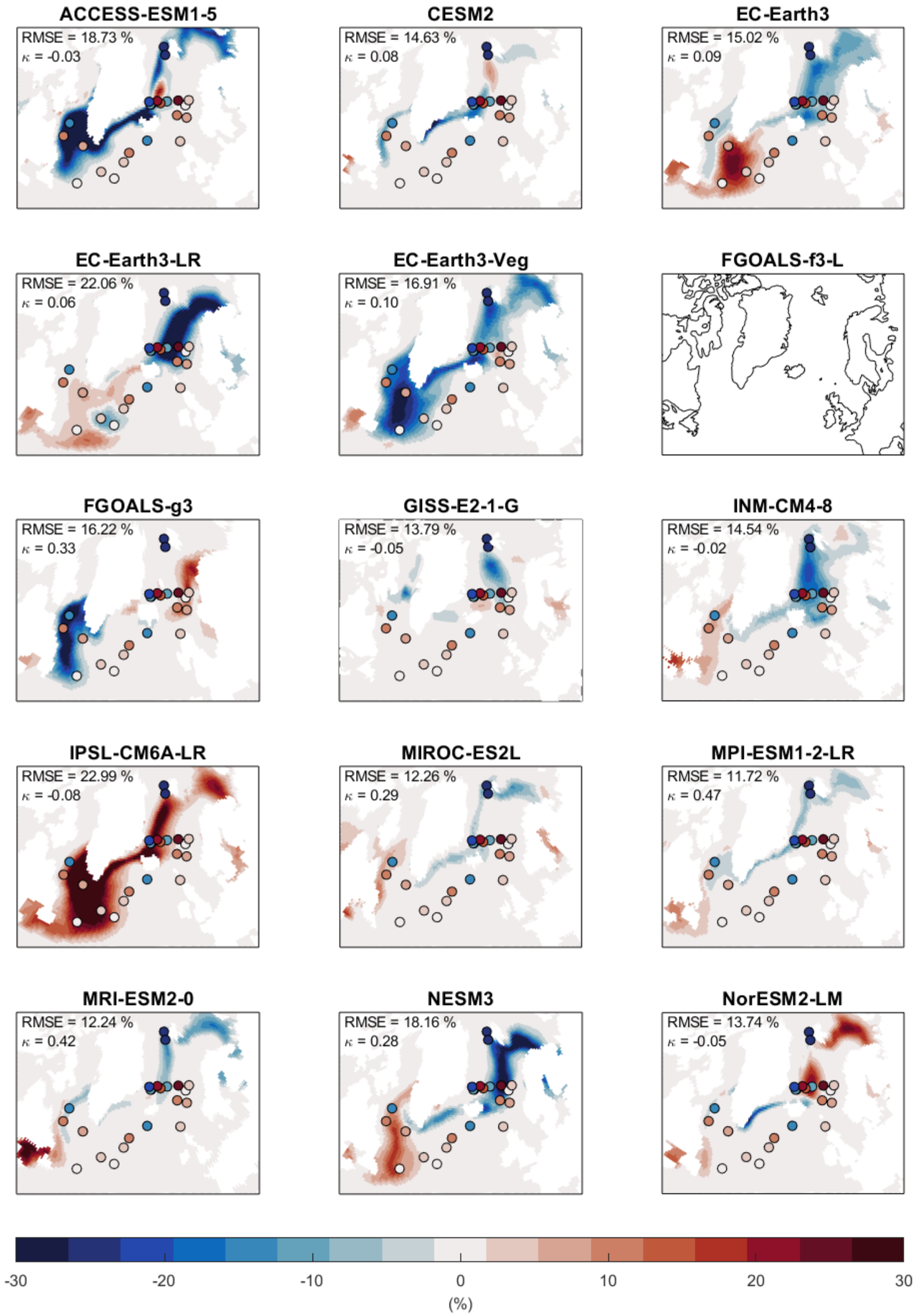

Figure S2. Changes in the winter sea ice concentration (MH-PI). Note that the PI sea ice concentration data is not available from FGOALS-f3-L.

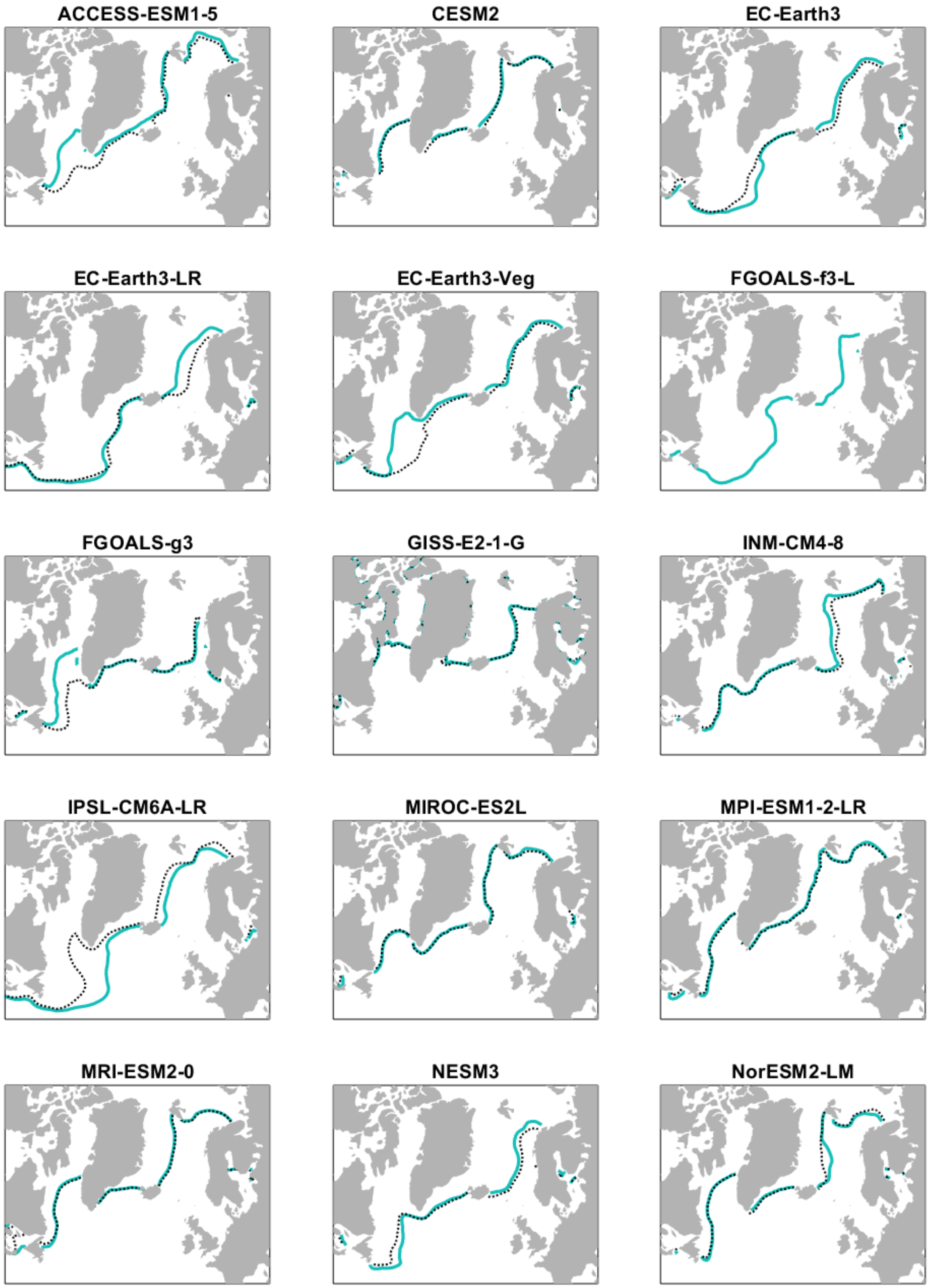

Figure S3. Winter sea ice extent in PI (black dotted line) and MH (green solid line), defined as the contour of 15% sea ice concentration. Note that the PI sea ice concentration data is not available from FGOALS-f3-L.

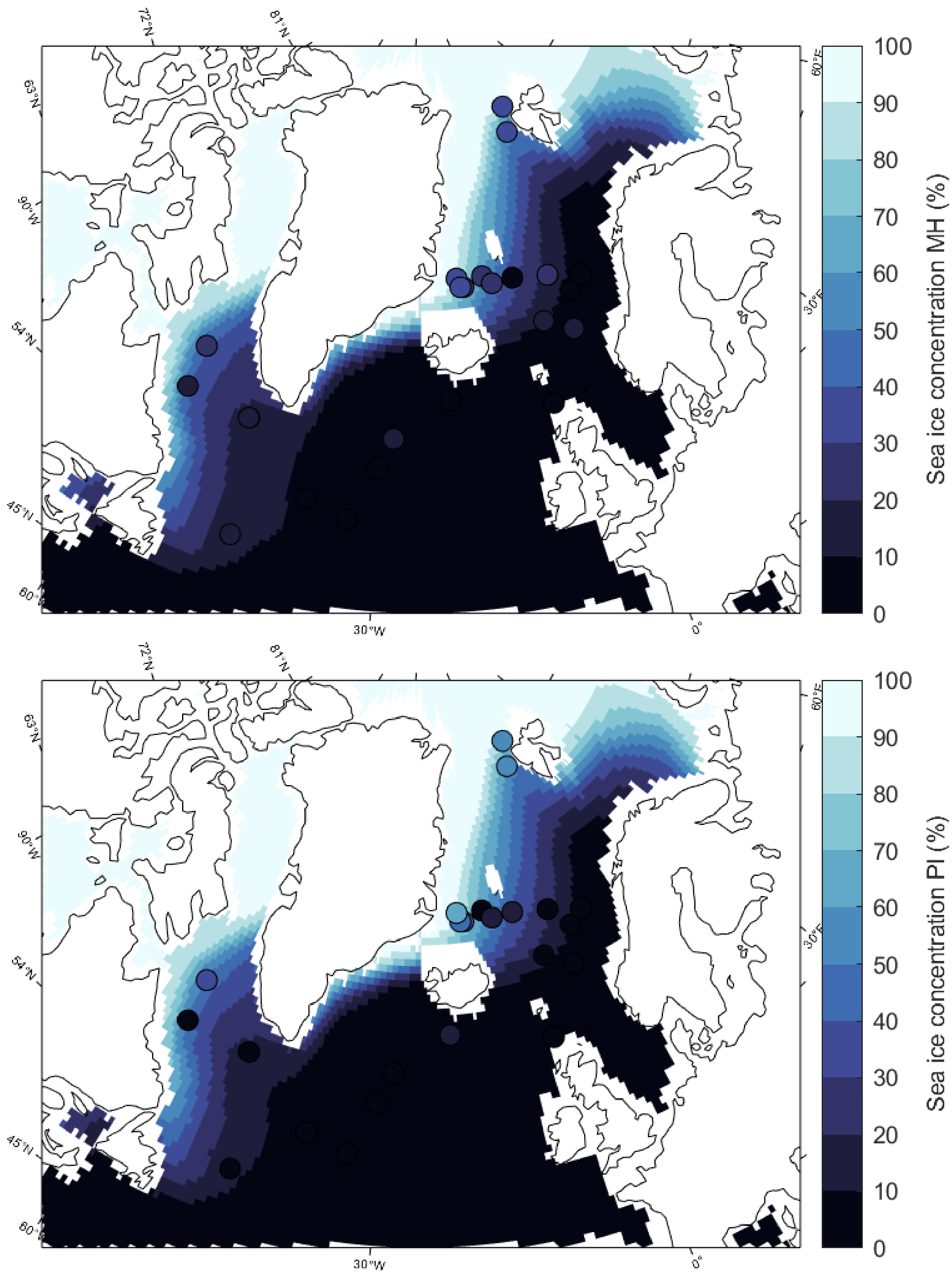

Figure S4. Winter (January to March) sea ice concentration of MH (top) and PI (bottom) from the PMIP4 model ensemble mean (background) versus proxy data (dots).

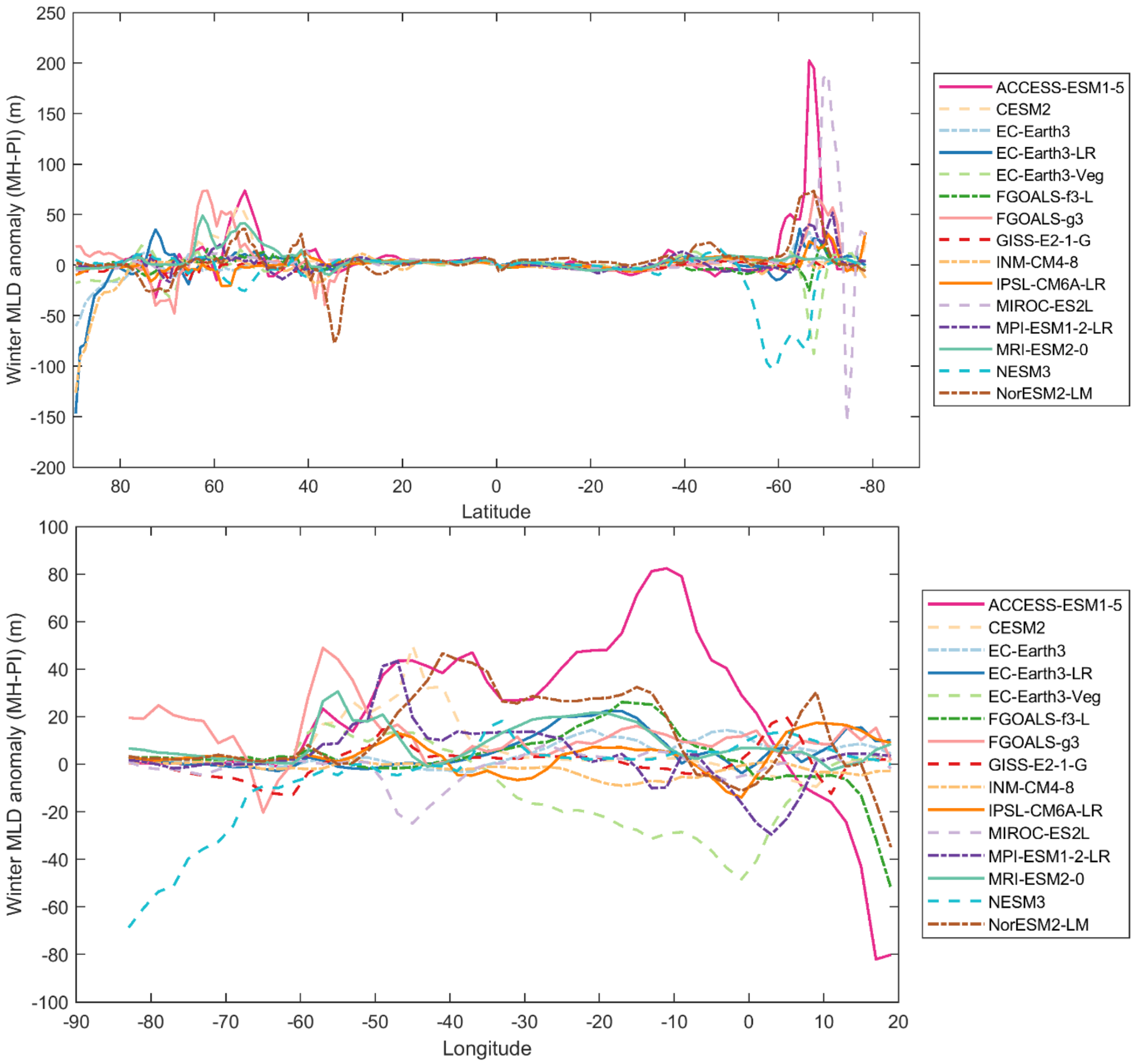

Figure S5. Zonal and meridional mean winter MLD anomaly (MH-PI).

Table S1. Summary of statistical metrics.

Model	RMSE	Spearman rho	Spearman p-value	Cohen's kappa	lower	upper
Mixed layer depth, winter (m) – PMIP4						
ACCESS-ESM1-5	273.04	-0.042	0.845	0.3469	-0.0043	0.6981
CESM2	127.60	-0.558	0.005	-0.3241	-0.7003	0.0521
EC-Earth3	80.53	0.085	0.694	0.0069	-0.3876	0.4014
EC-Earth3-LR	133.22	0.027	0.902	0.0204	-0.3573	0.3981
EC-Earth3-Veg	128.93	-0.147	0.492	-0.0070	-0.4070	0.3930
FGOALS-f3-L	74.64	0.118	0.582	-0.1126	-0.4258	0.2006
FGOALS-g3	363.36	-0.432	0.035	-0.2162	-0.5803	0.1478
GISS-E2-1-G	106.67	0.134	0.534	0.2703	-0.0776	0.6182
INM-CM4-8	76.84	-0.040	0.851	-0.2162	-0.5803	0.1478
IPSL-CM6A-LR	107.79	0.242	0.254	0.0571	-0.3301	0.4444
MIROC-ES2L	87.40	0.013	0.953	-0.1126	-0.4258	0.2006
MPI-ESM1-2-LR	106.04	-0.028	0.896	-0.0541	-0.4206	0.3125
MRI-ESM2-0	189.45	-0.064	0.767	0.4400	0.1507	0.7293
NESM3	95.85	-0.089	0.679	0.1367	-0.2386	0.5120
NorESM2-LM	150.05	0.120	0.575	-0.0070	-0.4070	0.3930
Ensemble	107.17	-0.154	0.471	0.0959	-0.2891	0.4809
Sea ice concentration, winter (%) – PMIP4						
ACCESS-ESM1-5	18.73	0.101	0.640	-0.0345	-0.2226	0.1536
CESM2	14.63	-0.154	0.472	0.0833	-0.3027	0.4694
EC-Earth3	15.02	-0.206	0.334	0.0943	-0.2153	0.4040
EC-Earth3-LR	22.06	-0.277	0.191	0.0588	-0.2907	0.4083
EC-Earth3-Veg	16.91	0.227	0.286	0.1034	-0.0427	0.2496
FGOALS-g3	16.22	0.274	0.195	0.3333	0.0767	0.5900
GISS-E2-1-G	13.79	-0.361	0.083	-0.0476	-0.4244	0.3292
INM-CM4-8	14.54	0.045	0.835	-0.0182	-0.2955	0.2591
IPSL-CM6A-LR	22.99	0.005	0.981	-0.0811	-0.2318	0.0696
MIROC-ES2L	12.26	0.270	0.202	0.2889	-0.1038	0.6816
MPI-ESM1-2-LR	11.72	0.525	0.009	0.4667	0.1015	0.8318
MRI-ESM2-0	12.24	0.134	0.531	0.4167	0.0645	0.7688
NESM3	18.16	-0.086	0.690	0.2800	-0.0656	0.6256
NorESM2-LM	13.74	0.104	0.628	-0.0476	-0.4244	0.3292
Ensemble	13.13	0.000	0.998	0.2453	-0.0476	0.5382
Mixed layer depth, winter (m) – PMIP3						
Model	RMSE	Spearman rho	Spearman p-value	Cohen's kappa	lower	upper
bcc-csm1-1	99.21	-0.532	0.007	-0.5616	-0.8974	-0.2258
CNRM-CM5	228.40	-0.196	0.358	-0.1126	-0.4258	0.2006

CSIRO-Mk3L-1-2	78.35	0.119	0.581	0.2500	-0.1360	0.6360
FGOALS-g2	130.71	-0.336	0.108	-0.2886	-0.6373	0.0601
FGOALS-s2	365.34	0.068	0.751	-0.0833	-0.4806	0.3140
GISS-E2-R	668.71	-0.375	0.071	0.0464	-0.2600	0.3528
HadGEM2-CC	119.44	-0.343	0.101	-0.2676	-0.6472	0.1120
HadGEM2-ES	84.50	-0.250	0.239	-0.1842	-0.4751	0.1066
IPSL-CM5A-LR	92.10	0.045	0.835	-0.1915	-0.5740	0.1910
KCM1-2-2	639.89	0.158	0.461	0.2053	-0.0897	0.5003
MIROC-ESM	122.21	-0.191	0.372	-0.1126	-0.4258	0.2006
MPI-ESM-P	155.11	0.119	0.581	0.0464	-0.2600	0.3528
MRI-CGCM3	78.60	0.077	0.721	0.1837	-0.1856	0.5530
Ensemble	112.51	-0.075	0.727	0.1200	-0.2052	0.4452
Mixed layer depth, annual (m) – PMIP4 last deglaciation						
Model	RMSE	Spearman rho	Spearman p-value	Cohen's kappa	lower	upper
HadCM3_uniform	27.09	0.173	0.419	-0.0400	-0.4079	0.3279
HadCM3_routed	26.65	0.398	0.054	0.1489	-0.2429	0.5408
TraCE-21ka	28.55	0.127	0.553	0.1837	-0.1856	0.5530
MPI_Glac1D_P1	68.29	-0.168	0.432	-0.0182	-0.2955	0.2591
MPI_Glac1D_P2	101.55	-0.167	0.437	-0.0848	-0.2496	0.0801
MPI_Glac1D_P3	138.43	-0.021	0.921	-0.0848	-0.2496	0.0801
MPI_Ice6G_P1	51.36	-0.336	0.108	0.0509	-0.0502	0.1519
MPI_Ice6G_P2	96.45	-0.094	0.661	-0.3585	-0.7097	-0.0073
MPI_Ice6G_P3	89.46	-0.060	0.779	0.0435	-0.3561	0.4431

Table S2. List of PMIP4 datasets used in this study.

model	MH data access and metadata	MH data doi	PI data access and metadata	PI data doi
ACCESS-ESM 1.5	http://cera-www.dkrz.de/WDCC/meta/CMIP6/CMIP6.PMIP.CSIRO.ACCESS-ESM1-5.midHolocene.r1i1p1f1.Omon.so.gn.v20210422	http://doi.org/10.22033/ESGF/CMIP6.13704	http://cera-www.dkrz.de/WDCC/meta/CMIP6/CMIP6.CMIP.CSIRO.ACCESS-ESM1-5.piControl.r1i1p1f1.Omon.so.gn.v20210316	http://doi.org/10.22033/ESGF/CMIP6.4312
CESM 2	http://cera-www.dkrz.de/WDCC/meta/CMIP6/CMIP6.PMIP.NCAR.CESM2.midHolocene.r1i1p1f1.Omon.thetao.gn.v20190923	http://doi.org/10.22033/ESGF/CMIP6.7674	http://cera-www.dkrz.de/WDCC/meta/CMIP6/CMIP6.CMIP.NCAR.CESM2.piControl.r1i1p1f1.Omon.thetao.gn.v20190320	http://doi.org/10.22033/ESGF/CMIP6.7733
EC-Earth 3	http://cera-www.dkrz.de/WDCC/meta/CMIP6/CMIP6.PMIP.EC-Earth-Consortium.EC-Earth3.midHolocene.r1i1p1f1.Omon.so.gn.v20231010	http://doi.org/10.22033/ESGF/CMIP6.11224	http://cera-www.dkrz.de/WDCC/meta/CMIP6/CMIP6.CMIP.EC-Earth-Consortium.EC-Earth3.piControl.r1i1p1f1.Omon.thetao.gn.v20200918	http://doi.org/10.22033/ESGF/CMIP6.4842
EC-Earth 3-LR	http://cera-www.dkrz.de/WDCC/meta/CMIP6/CMIP6.PMIP.EC-Earth-Consortium.EC-Earth3-LR.midHolocene.r1i1p1f1.Omon.so.gn.v20200919	http://doi.org/10.22033/ESGF/CMIP6.4801	http://cera-www.dkrz.de/WDCC/meta/CMIP6/CMIP6.CMIP.EC-Earth-Consortium.EC-Earth3-LR.piControl.r1i1p1f1.Omon.so.gn.v20200919	http://doi.org/10.22033/ESGF/CMIP6.4847
EC-Earth 3-Veg	http://cera-www.dkrz.de/WDCC/meta/CMIP6/CMIP6.PMIP.EC-Earth-Consortium.EC-Earth3-Veg.midHolocene.r1i1p1f1.Omon.so.gn.v20231010	http://doi.org/10.22033/ESGF/CMIP6.18105	http://cera-www.dkrz.de/WDCC/meta/CMIP6/CMIP6.CMIP.EC-Earth-Consortium.EC-Earth3-Veg.piControl.r1i1p1f1.Omon.so.gn.v20210419	http://doi.org/10.22033/ESGF/CMIP6.4848
FGOALS-f3-L	http://cera-www.dkrz.de/WDCC/meta/CMIP6/CMIP6.PMIP.CAS.FGOALS-f3-L.midHolocene.r1i1p1f1.Omon.so.gn.v20191031	http://doi.org/10.22033/ESGF/CMIP6.12014	http://cera-www.dkrz.de/WDCC/meta/CMIP6/CMIP6.CMIP.CAS.FGOALS-f3-L.piControl.r1i1p1f1.Omon.thetao.gn.v20191028	http://doi.org/10.22033/ESGF/CMIP6.3447

FGOALS-g3	http://cera-www.dkrz.de/WDCC/meta/CMIP6/CMIP6.PMIP.CAS.FGOALS-g3.midHolocene.r1i1p1f1.Omon.thetao.gn.v20191025	http://doi.org/10.22033/ESGF/CMIP6.3409	http://cera-www.dkrz.de/WDCC/meta/CMIP6/CMIP6.CMIP.CAS.FGOALS-g3.piControl.r1i1p1f1.Omon.so.gn.v20191126	http://doi.org/10.22033/ESGF/CMIP6.3448
GISS-E2.1G	http://cera-www.dkrz.de/WDCC/meta/CMIP6/CMIP6.PMIP.NASA-GISS.GISS-E2-1-G.midHolocene.r1i1p1f1.Omon.so.gn.v20190916	http://doi.org/10.22033/ESGF/CMIP6.7225	http://cera-www.dkrz.de/WDCC/meta/CMIP6/CMIP6.CMIP.NASA-GISS.GISS-E2-1-G.piControl.r1i1p1f1.Omon.thetao.gn.v20180824	http://doi.org/10.22033/ESGF/CMIP6.7380
INM-CM4-8	http://cera-www.dkrz.de/WDCC/meta/CMIP6/CMIP6.PMIP.INM.INM-CM4-8.midHolocene.r1i1p1f1.Omon.thetao.gr1.v20190802	http://doi.org/10.22033/ESGF/CMIP6.5077	http://cera-www.dkrz.de/WDCC/meta/CMIP6/CMIP6.CMIP.INM.INM-CM4-8.piControl.r1i1p1f1.Omon.so.gr1.v20190605	http://doi.org/10.22033/ESGF/CMIP6.5080
IPSL-CM6A-LR	http://cera-www.dkrz.de/WDCC/meta/CMIP6/CMIP6.PMIP.IPSL.IPSL-CM6A-LR.midHolocene.r1i1p1f1.Omon.so.gn.v20180926	http://doi.org/10.22033/ESGF/CMIP6.5229	http://cera-www.dkrz.de/WDCC/meta/CMIP6/CMIP6.CMIP.IPSL.IPSL-CM6A-LR.piControl.r1i1p1f1.Omon.so.gn.v20200326	http://doi.org/10.22033/ESGF/CMIP6.5251
MIROC-ES2L	http://cera-www.dkrz.de/WDCC/meta/CMIP6/CMIP6.PMIP.MIROC.MIROC-ES2L.midHolocene.r1i1p1f2.Omon.thetao.gn.v20191002	http://doi.org/10.22033/ESGF/CMIP6.5646	http://cera-www.dkrz.de/WDCC/meta/CMIP6/CMIP6.CMIP.MIROC.MIROC-ES2L.piControl.r1i1p1f2.Omon.so.gn.v20190823	http://doi.org/10.22033/ESGF/CMIP6.5710
MPI-ESM1.2-LR	http://cera-www.dkrz.de/WDCC/meta/CMIP6/CMIP6.PMIP.MPI-M.MPI-ESM1-2-LR.midHolocene.r1i1p1f1.Omon.thetao.gn.v20190710	http://doi.org/10.22033/ESGF/CMIP6.6644	http://cera-www.dkrz.de/WDCC/meta/CMIP6/CMIP6.CMIP.MPI-M.MPI-ESM1-2-LR.piControl.r1i1p1f1.Omon.so.gn.v20190710	http://doi.org/10.22033/ESGF/CMIP6.6675

MRI-ESM2.0	http://cera-www.dkrz.de/WDCC/meta/CMIP6/CMIP6.PMIP.MRI.MRI-ESM2-0.midHolocene.r1i1p1f1.Omon.thetao.gn.v20210525	http://doi.org/10.22033/ESGF/CMIP6.6860	http://cera-www.dkrz.de/WDCC/meta/CMIP6/CMIP6.CMIP.MRI.MRI-ESM2-0.piControl.r1i1p1f1.Omon.so.gn.v20210311	http://doi.org/10.22033/ESGF/CMIP6.6900
NESM v3	http://cera-www.dkrz.de/WDCC/meta/CMIP6/CMIP6.PMIP.NUIST.NESM3.midHolocene.r1i1p1f1.Omon.thetao.gn.v20190926	http://doi.org/10.22033/ESGF/CMIP6.8773	http://cera-www.dkrz.de/WDCC/meta/CMIP6/CMIP6.CMIP.NUIST.NESM3.piControl.r1i1p1f1.Omon.so.gn.v20190704	http://doi.org/10.22033/ESGF/CMIP6.8776
NorESM2-LM	http://cera-www.dkrz.de/WDCC/meta/CMIP6/CMIP6.PMIP.NCC.NorESM2-LM.midHolocene.r1i1p1f1.Omon.thetao.gr.v20191108	http://doi.org/10.22033/ESGF/CMIP6.8079	http://cera-www.dkrz.de/WDCC/meta/CMIP6/CMIP6.CMIP.NCC.NorESM2-LM.piControl.r1i1p1f1.Omon.thetao.gr.v20210118	http://doi.org/10.22033/ESGF/CMIP6.8217